Mathematical Statistician and Engineering Applications
ISSN: 2094-0343
2326-9865

# Analysis of Signals with Parasitic Phase Modulation in Signal Generators Based on DDS with Phase Distortion Autocompensation for Geoecological Monitoring Systems

Phd., associate Professor Gleb S. Vasilyev[1]

Phd., associate Professor Dmitry I. Surzhik[1,2]

D.Sc. in Engineering, Professor Oleg R. Kuzichkin[1]

[1]Belgorod State Research University, Russia

[2]Vladimir State University named after Alexander G. and Nikolai G. Stoletovs, Russia

**Article Info**
**Page Number: 957 – 966**
**Publication Issue:**
**Vol. 71 No. 3s2 (2022)**

**Article History**
**Article Received:** 28 April 2022
**Revised:** 15 May 2022
**Accepted:** 20 June 2022
**Publication:** 21 July 2022

**Abstract** – A block diagram of a signal generator based on a direct digital synthesizer with automatic phase distortion compensation for geoecological monitoring systems is considered. Analytical expressions of an arbitrary deterministic signal with single-tone phase modulation and its spectrum based on piecewise linear approximation and mathematical apparatus of Bessel functions are obtained. The amplitude spectrum of a phase-modulated periodic sequence of unipolar exponential pulses is calculated at two values of the modulation index. The results obtained describe transient processes on the output of a two-half-period rectifier in the information path of an autocompensator and can be used to analyze the effect of parasitic phase modulation (jitter) on the operating mode of the device.
**Keywords** – agro-industrial complex, signal generators, digital computing synthesizers, automatic compensation, parasitic phase modulation.

## Introduction

Currently, the study of geodynamic processes and phenomena [1-3] occurring in the upper near-surface part of the geological environment developed by the branches of the agro-industrial complex and bearing both natural and man-made character is becoming more and more relevant. The interest in the research of emerging movements and deformations of the geological environment is largely due to the fact that the safe conduct of human economic activity in the territories of the agro-industrial complex is possible only when obtaining a complete picture of the processes occurring on the surface and in the subsurface. The study of geodynamic process data requires high-precision measurements in the monitoring mode using modern high-current and productive geophysical equipment. As a result, modern geodynamic monitoring systems are complex software and hardware complexes based on various physical phenomena and effects [4-6]. One of the promising options for the implementation of geodynamic monitoring at the local level is the use of modern systems based on the geoelectric control methods. In various modifications of geoelectrics methods (over fifty), probing signals are applied to point emitting grounding electrodes placed in the geological environment in a controlled area.

To form probing signals in geodynamic monitoring systems, various generating equipment is currently used, and the signal generators work, as a rule, in a narrow range of time, on a limited set of their values and are not universal. Another shortcoming of modern signal generators of geodynamic monitoring systems based on geoelectric control methods is associated with the need to detect small geodynamic changes in the near-surface zones of the geological environment and the initial signs of possible catastrophic processes. In this aspect, the spectral purity of the synthesized signals becomes an important parameter.

Signal generator for geodynamic monitoring systems of agricultural resources based on direct digital synthesizers (DDS) with automatic phase distortion compensation

Based on the features and requirements imposed on the radiating paths of the geodynamic monitoring system of agricultural resources based on geoelectric control methods, the most attractive from a practical point of view option for implementing a universal signal generator is its construction based DDS [7, 8]. This approach allows for high accuracy of synthesized signals, extremely high frequency resolution (up to thousandths of a hertz), high switching speed, ease of control and the possibility of forming complex signals. At the same time, obtaining probing signals with the required parameters will be achieved by promptly changing the amplitude, frequency and phase control codes on a real-time scale.

However, among the disadvantages of the DDS, a significant level of discrete parasitic spectral components of the output signal should be noted. To improve the spectral characteristics of DDS as signal generators of geodynamic monitoring systems based on geoelectric control methods, it is proposed to use the method of automatic phase distortion compensation (APDC) [9, 10]. In general, this method is based on the isolation of phase distortions present in the output signal of an arbitrary radio device by their phase detection relative to the signal without distortion and subsequent compensation in automatic mode. The most important advantages of this method in relation to DDS over traditional (filtering and randomization) are the following features:

- it allows to reduce the most undesirable spectral components (located in the near zone of the fundamental frequency of the synthesized oscillation) arising from several sources;
- has selective properties with respect to the useful modulation of the output signal;
- does not require adjustment of the autocompensator units when changing the parameters of the device.

Theoretical and experimental research of this method has shown the effectiveness of autocompensation and the possibility of improving the spectral characteristics of DDS by 10-15 dB.

As an autocompensator control device in the frequency range up to several tens of MHz, it is easiest to use a controlled phase shifter, the reduction of phase distortion in which is based on the antiphase modulation of the input or output signal of the DDS in accordance with the control signal of the autocompensator. Depending on the particular point of the circuit information where phase distortions are present, several types of auto-compensators can be used: with forward regulation, backward regulation and combined regulation.

The block diagram of the signal generator variant for geodynamic monitoring systems of agro-industrial complex resources based on DDS with APDC and backward control is shown in Fig. 1. Here the autocompensator includes a delay control device (DCD) based on a controlled phase shifter, a reference path (RP), an information path (IP), a control path (CP) and

phase detector (PD). Also, the following designations are adopted in the scheme: RG - reference generator, FC –frequency converter (multiplier or divider), digital-analog converter (DAC) and low-pass filter (LPF).

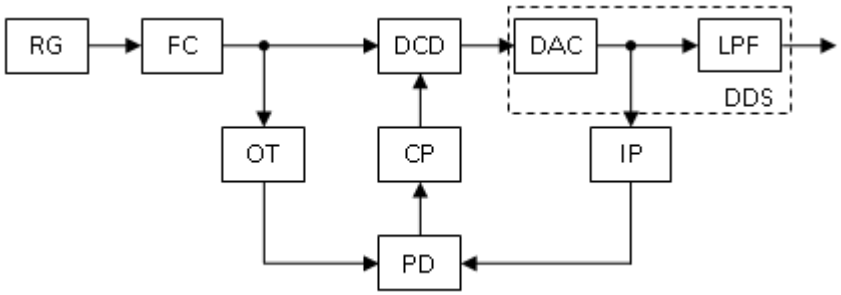


Fig. 1 – Block diagram of a signal generator for geodynamic monitoring systems based on DDS with APDC and backward regulation

The principle of operation of the circuit is based on the fact that the reference and information paths form input pulses for the phase detector having the same frequency and different phase shifts. These paths include differentiating circuits and T-triggers that directly generate pulses from positive voltage surges and divide their input frequency by two. In addition, a full-wave rectifier at the output of the differentiating circuit of the information path converts input multipolar voltage surges into unipolar ones, which are transmitted to the input of the corresponding T-trigger. The control path of the autocompensator consists of a low-pass filter and an amplifier. The parasitic phase deviation directly allocated in the control path is compensated by an antiphase change in the delay of the reference signal in the delay control device.

**Problem setup**

In the analytical study of the transient modes of a signal generator with APDC, it is necessary to obtain expressions for the signals of its control path, as well as their spectra. With variations in the parameters of the autocompensator and the presence of parasitic phase modulation of the studied signals (even in the simplest case of single-tone modulation), obtaining analytical expressions for the spectra of the control path signals is generally difficult or impossible. Thus, in [11], an analytical representation of a periodic sequence of rectangular pulses with single-tone phase modulation by a Fourier series was performed and the spectral composition of the modulated sequence was analyzed using Bessel functions.

With regard to the studied autocompensator, these results are only valid for rectangular signals at the output of T-triggers. When analyzing the spectra of other PM signals of a more complex form (for example, exponential pulses at the outputs of differentiating circuits or a full-wave rectifier), analytical solutions are generally absent, so we have to resort to numerical methods.

The authors proposed an approximation of arbitrary deterministic effects based on continuous piecewise linear functions (CPLF) and performed an analytical calculation of the transient modes of various radio signal converters by the spectral method [12-15]. It seems possible to generalize this approach also for PM signals.

**Solution**

Approximation of an arbitrary deterministic signal s(t) based on CPLF has the form [13]

$$s(t)=\sum_{k=0}^{K-1}s_k(t)=\sum_{k=0}^{K-1}(K_k t+B_k)Q_k(t),$$

(1)

where k, K are the current and maximum number of the approximation node, $K_k=\frac{s(t_{k+1})-s(t_k)}{\Delta t_k}$ and $B_k=s(t_k)-K_k t_k$ are approximation coefficients, $\Delta t_k=t_{k+1}-t_k$ is approximation step, $Q_k(t)$ is CPLF of inclusion equal to 1 in the interval $t_k<t<t_{k+1}$ and equal to 0 outside the interval. When analyzing a periodic signal, it is advisable to choose the approximation range [$t_0$; $t_K$] equal to the period of the signal under study.

In general, the spectrum of a signal s(t) with a period T based on the Fourier series expansion has the form [16, 17]:

$$c_n=\frac{1}{T}\int_{-T/2}^{T/2}s(t)\cdot\cos(n\omega_1 t)dt-j\frac{1}{T}\int_{-T/2}^{T/2}s(t)\cdot\sin(n\omega_1 t)dt,$$

(2)

where $\omega_1=2\pi/T$ is the frequency of the signal.

Using (1), we represent the spectrum (2) by the sum of the spectra

$$c_n=\sum_{k=0}^{K-1}c_{n,k}=\frac{1}{T}\int_{-T/2}^{T/2}s_k(t)\cdot\cos(n\omega_1 t)dt-j\frac{1}{T}\int_{-T/2}^{T/2}s_k(t)\cdot\sin(n\omega_1 t)dt.$$

(3)

After the time shift of the approximating segment $K_k t+B_k$ to the left by $t_k^*=t_k+\Delta t_k/2$, this segment is shifted from the interval $t_k<t<t_{k+1}$ to the new interval . Thus, the expression $K_k t+B_k$ in the new interval is the sum of an odd function $K_k t$ and an even function $B_k$. This makes it possible to equate to zero the corresponding cosine (for $K_k t$) and the sine (for $B_k$) term of (3) and simplify the resulting expressions. Substituting (1) into (3), for the k-th segment we get

$$c_{n,k}=\left[a_{n,k}-jb_{n,k}\right]e^{-jn\omega_1 t_k^*}=\left[\frac{1}{T}\int_{-\Delta t_k/2}^{\Delta t_k/2}B_k\cos(n\omega_1 t)dt-j\frac{1}{T}\int_{-\Delta t_k/2}^{\Delta t_k/2}K_k t\sin(n\omega_1 t)dt\right]e^{-jn\omega_1 t_k^*},$$

(4)

The multiplier $e^{-jn\omega_1 t_k^*}$ takes into account the time shift by $t_k^*$.

Having calculated the coefficients (4) and denoting $q_{0k}=\frac{T}{\Delta t_k}$ - the inversed fill-factor of the periodic sequence of approximating pulses with the number k, we define the Fourier series in trigonometric form as

$$s_k\left(t+t_k^*\right)=\frac{a_{0,k}}{2}+\sum_{n=1}^{\infty}a_{n,k}\cos(n\omega_1 t)+b_{n,k}\sin(n\omega_1 t),$$

(5)

where $a_0 = \frac{2B_k}{q_{0k}}$, $a_{n,k} = \frac{2B_k}{n\pi}\sin\frac{n\pi}{q_{0k}}$, $b_{n,k} = \frac{K_k}{n\pi}\left(\frac{1}{n\pi}\sin\frac{n\pi}{q_{0k}} - \frac{1}{q_{0k}}\cos\frac{n\pi}{q_{0k}}\right)$.

We assume that the time shift of the approximating segments (pulses) is proportional to the values of the modulating signal at the approximation nodes, which is equivalent to phase pulse modulation of the second kind (PPM-2) of the original (modulating) signal. In this case, the magnitude of the time shift of the k-th pulse relative to the node $t_k$ is determined by the formula $\Delta\tau_k(t) = \Delta\tau_{макс}\sin\omega_м t$, where $\Delta\tau_{макс}$ is the maximum time shift, $\omega_m$ is the frequency of phase modulation.

The current phase of the phase-modulated signal is determined by value $\Delta\tau_k$ and frequency of the original signal $\omega_1$:

$$\theta(t) = \omega_1 t + \Delta\varphi_{\max}\sin\omega_m t,$$

(6)

where $\Delta\varphi_{\max} = \Delta\tau_{\max}\omega_1$ is the modulation index.

The instantaneous frequency of the PPM signal will be equal to

$$\omega_{inst} = \frac{d\theta(t)}{dt} = \omega_1 + \Delta\varphi_{\max}\omega_m\cos\omega_m t.$$

(7)

When substituting into formula (5) instead of $\omega_1 t$ the value $\theta(t)$ from (6) and instead of T – the value $T_{inst} = 2\pi/\omega_{inst}$ from (7), we obtain an expression for the PPM signal:

$$\begin{aligned}\tilde{s}_k\left(t+t_k^*\right) &= \frac{B_k}{q_{0k}}\left(1+\Delta\tau_{\max}\omega_m\cos\omega_m t\right)+\\ &+\frac{2B_k}{\pi}\sum_{n=1}^{\infty}\frac{1}{n}\sin\frac{n\pi}{q_{0k}}\left(1+\Delta\tau_{\max}\omega_m\cos\omega_m t\right)\cos n\omega_1\left(t+\Delta\tau_{\max}\sin\omega_m t\right)+\\ &+\frac{K_k}{\pi}\sum_{n=1}^{\infty}\frac{1}{n}\left[\frac{1}{n\pi}\sin\frac{n\pi}{q_{0k}}\left(1+\Delta\tau_{\max}\omega_m\cos\omega_m t\right)-\frac{1}{q_{0k}}\cos\frac{n\pi}{q_{0k}}\left(1+\Delta\tau_{\max}\omega_m\cos\omega_m t\right)\right]\times\\ &\times\sin n\omega_1\left(t+\Delta\tau_{\max}\sin\omega_m t\right).\end{aligned}$$

(8)

Using the property of the Bessel functions [9] $J_l(\beta)$ [9]

$$\sin(\alpha+\beta\sin\phi) = \sum_{l=-\infty}^{\infty}J_l(\beta)\sin(\alpha+l\phi),$$

(9)

we transform (8) and signify the finite upper limits of the sums as L and N:

$$\begin{aligned}\tilde{s}_k\left(t+t_k^*\right) &= \frac{B_k}{q_{0k}}\left(1+\Delta\tau_{\max}\omega_m\cos\omega_m t\right)+\\ &+\frac{2B_k}{\pi}\sum_{n=1}^{N}\frac{1}{n}\sin\frac{n\pi}{q_{0k}}\sum_{l=0}^{L}J_l(n\Delta\varphi_{\max})\cos(n\omega_1\pm l\omega_m)t+\\ &+\frac{K_k}{\pi q_{0k}}\sum_{n=1}^{\infty}\frac{1}{n}\left(\frac{q_{0k}}{n\pi}\sin\frac{n\pi}{q_{0k}}-\cos\frac{n\pi}{q_{0k}}\right)\sum_{l=0}^{L}J_l(n\Delta\varphi_{\max})\sin(n\omega_1\pm l\omega_m)t.\end{aligned}$$

(10)

As follows from formula (10), the spectral composition of one segment of the approximation of PPM signal (1) includes: a constant component with amplitude $A_{0k} = \frac{B_k}{q_{0k}}$, a signal with phase modulation frequency $\omega_м$ and amplitude $A_{i\,k} = \frac{B_k}{q_{0k}} \Delta\tau_{\max} \omega_m$, harmonics of the frequency of the original signal $\omega_1$, as well as lower and upper side frequencies $n\omega_1 \pm l\omega_м$. The arrangement of harmonics in the signal spectrum (10) is identical to that presented in [11] for the PM sequence of rectangular pulses, only the amplitudes of harmonics differ.

We apply the following designation into (10): $B^*_{k,n,l} = \frac{2B_k}{n\pi} \sin\frac{n\pi}{q_{0k}} J_l(n\Delta\varphi_{\max})$, $K^*_{k,n,l} = \frac{K_k}{n\pi q_{0k}} \left( \frac{q_{0k}}{n\pi} \sin\frac{n\pi}{q_{0k}} - \cos\frac{n\pi}{q_{0k}} \right) J_l(n\Delta\varphi_{\max})$ are the amplitudes of the odd and even component of the signal with frequencies $\omega_{n,l} = n\omega_1 \pm l\omega_m$, thus we obtain

$$\tilde{s}_k\left(t + t^*_k\right) = A_{0k} + A_{i\,k} \cos\omega_m t + \sum_{n=1}^{N} \sum_{l=0}^{L} B^*_{k,n,l} \cos\omega_{n,l} t + K^*_{k,n,l} \sin\omega_{n,l} t.$$

(10)

Based on (11), summing over all k=0…K-1 we obtain

$$\tilde{s}(t) = \sum_{k=0}^{K-1} \tilde{s}_k\left(t\right) = A_0 + \sum_{k=0}^{K-1} A_{м\,k} \cos\omega_м\left(t - t^*_k\right) +$$

$$+ \sum_{k=0}^{K-1} \sum_{n=1}^{N} \sum_{l=0}^{L} B^*_{k,n,l} \cos\omega_{n,l}\left(t - t^*_k\right) + K^*_{k,n,l} \sin\omega_{n,l}\left(t - t^*_k\right),$$

(12)

where $A_0 = \sum_{k=0}^{K-1} A_{0k}$ is the constant component of the PPM signal.

Using (12) and taking into account the time shift $-t^*_k$ by a multiplier $e^{jn\omega_1 t^*_k}$, we obtain expressions for the complex amplitudes of harmonics in the spectrum of the modulated signal:

$$S_i = \sum_{k=0}^{K-1} A_{mk} e^{jn\omega_1 t^*_k},\ S_{n,l} = \sum_{k=0}^{K-1} \left(B^*_{k,n,l} - jK^*_{k,n,l}\right) e^{jn\omega_1 t^*_k}.$$

(13)

According to the expression (12), the calculation of the pulse sequence at the output of a full-wave rectifier in the APDC information path is performed. A single pulse at the output of the rectifier after normalization in amplitude has the form $s_{FWR}(t) = \exp(-t / T_{DC2})$ where $T_{DC2}$ is the time constant preceding the rectifier according to the scheme of the differentiating circuit. The parameters of the signal under study are assumed to be equal: the number of approximation nodes K=6, the number of approximating segments K–1=5, the upper limits of the sums in (10) N=10, L=6, the modulation index and frequency $\Delta\varphi_{\max}$ =0.6 and $\omega_m$ =0.05$\omega_1$, the time constant $T_{DC2}$=0,05T.

The initial signal at the output of the full-wave rectifier $s_{FWR}(t)$ and the modulated signal

$\tilde{s}_{FWR}(t)$, as well as the modulating signal $u_m(t) = \Delta\varphi_{\max} \sin \omega_m t$ are shown in Fig. 2. The amplitude spectra of the modulated signal, calculated by expressions (13) and $A_{m,n,l} = |S_{m,n,l}|$ with modulation indices $\Delta\varphi_{\max}$ = 0.2 and 0.6, respectively, are shown in Fig. 3 and 4.

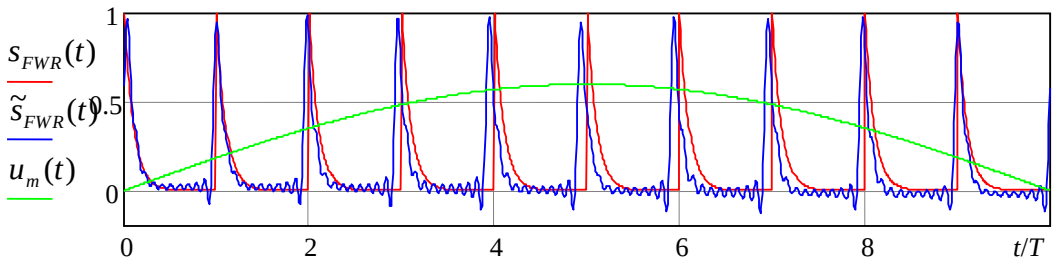


Fig. 2 The initial signal at the output of the full-wave rectifier $s_{FWR}(t)$, the modulated signal $\tilde{s}_{FWR}(t)$ and the modulating signal $u_m(t) = \Delta\varphi_{\max} \sin \omega_m t$

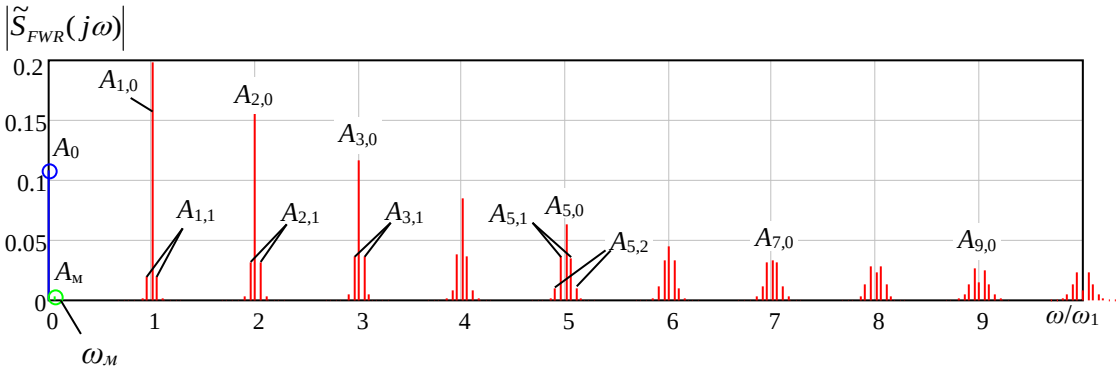


Fig. 3 – Amplitude spectrum of the phase–modulated signal $\tilde{s}_{FWR}(t)$, modulation index 0.2

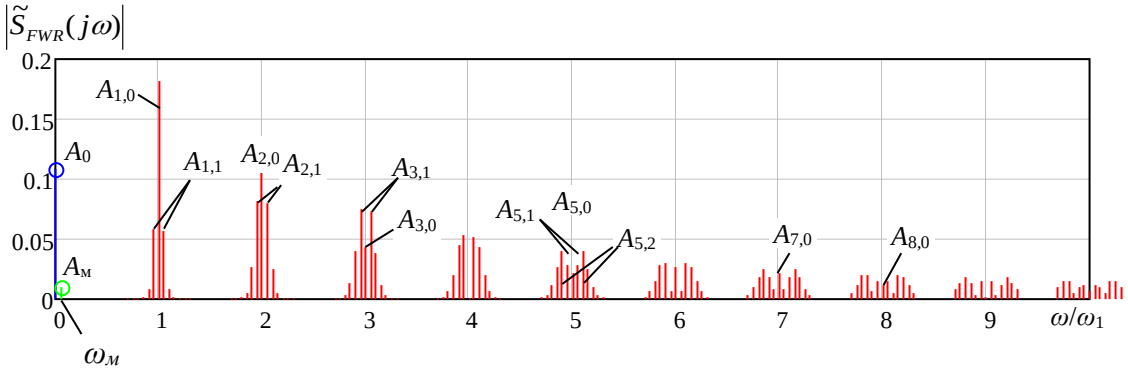


Fig. 4 – Amplitude spectrum of the phase–modulated signal $\tilde{s}_{FWR}(t)$, modulation index 0.6

**Conclusion**

A comparison of Figures 3 and 4 shows that an increase of $\Delta\varphi_{\text{ìàêñ}}$ leads to an expansion of the spectra near the harmonics of the sampling frequency $\omega_{n,0} = n\omega_1$ and an increase in the amplitude of the component with the modulation frequency $A_м$, the amplitude of the constant component remains the same ($A_0$=0.108). Checking the harmonic values (13), performed us-

ing the fast Fourier transform for the signal $\tilde{s}_{FWR}(t)$, showed an exact match of the calculated spectra (for multiple ratios of the sampling interval and the period of the modulating signal $T_m=2\pi/\omega_m=20T$).

The good accuracy of the representation of PM signal by formula (12) and its spectrum (13) confirms the validity of the proposed approach and the expressions obtained for the analysis of phase-modulated signals. The undulation of the curve $\tilde{s}_{FWR}(t)$ is due to the Gibbs effect.

The obtained results can be used for an analytical study of the modes of operation of signal generators for geodynamic monitoring systems of agro-industrial complex resources based on DDS with APDC, as well as other radio devices in the presence of parasitic phase modulation (jitter).

## Acknowledgements

The work was supported by the RFBR grant 19-29-06030-mk "Research and development of a wireless ad-hoc network technology between UAVs and control centers of the "smart city" based on the adaptation of transmission mode parameters at different levels of network interaction". The theory was prepared within the framework of the state task of the Russian Federation FZWG-2020-0029 "Development of theoretical foundations for building information and analytical support for telecommunications systems for geoecological monitoring of natural resources in agriculture".

## References

1. Korolev V.A. Monitoring of the geological environment / Moscow: Publishing House of Moscow State University. - 1995.
2. Turcotte, D.; Schubert, G. (2002). Geodynamics (2nd ed.). New York: Cambridge University Press.
3. Jolivet, Laurent; Nataf, Henri-Claude; Aubouin, Jean (1998). Geodynamics. Taylor & Francis. ISBN 9789058092205.
4. Vanitha, D. D. . (2022). Comparative Analysis of Power switches MOFET and IGBT Used in Power Applications. International Journal on Recent Technologies in Mechanical and Electrical Engineering, 9(5), 01–09. https://doi.org/10.17762/ijrmee.v9i5.368
5. Pozdnyakov A.I., Gulalyev S.G. Electrophysical properties of several soils / Moscow-Baku "Adiloglu". - 2004. – 240 p.
6. Khmelevsky V.K. Electrical exploration. Handbook of Geophysics in two books. Edited by V.K. Khmelevsky and V.M. Bondarenko. - 2nd edition. - Moscow: Nedra, 1989.
7. Deepak Mathur, N. K. V. . (2022). Analysis & Prediction of Road Accident Data for NH-19/44. International Journal on Recent Technologies in Mechanical and Electrical Engineering, 9(2), 13–33. https://doi.org/10.17762/ijrmee.v9i2.366
8. Khmelevsky V.K. Electical investigation by the method of resistances. / Edited by V.K. Khmelevsky: Textbook. – M.: Publishing House of Moscow State University, 1994. 160 p.

9. Malla, S., M. J. . Meena, O. . Reddy. R, V. . Mahalakshmi, and A. . Balobaid. “A Study on Fish Classification Techniques Using Convolutional Neural Networks on Highly Challenged Underwater Images”. International Journal on Recent and Innovation Trends in Computing and Communication, vol. 10, no. 4, Apr. 2022, pp. 01-09, doi:10.17762/ijritcc.v10i4.5524.
10. Krupa, V.F. Contours of phase synchronization and frequency synthesis / V.F. Krupa. - John Wiley & Sons, Ltd. -2003. – 320 p.
11. Jouko Vankka & Kari A.I. Halonen (2010). Direct Digital Synthesizers: Theory, Design and Applications. The Kluwer international series in Engineering and Computer Science. Boston, MA: Kluwer Academic Publishers.
12. Surzhik D.I., Vasiliev G.S., Kuzichkin O.R. The use of phase distortion autocompensation to improve the spectral characteristics of signal generators of radio transmitters of unmanned aerial vehicles / International Journal of Engineering Research and Technology. Volume 13, Issue 11. – 2020. – pp. 3778-3782.
13. Tume-Bruce, B. A. A. ., A. . Delgado, and E. L. . Huamaní. “Implementation of a Web System for the Improvement in Sales and in the Application of Digital Marketing in the Company Selcom”. International Journal on Recent and Innovation Trends in Computing and Communication, vol. 10, no. 5, May 2022, pp. 48-59, doi:10.17762/ijritcc.v10i5.5553.
14. Dorofeev NV, Grecheneva AV Kuzichkin OR, Surzhik DI, Romanov RV. The method and devices of autocompensation of phase distortions of direct digital synthesizers of signal formers of georadars / 2018 2ND International conference on functional materials and chemical engineering (ICFMCE 2018), series of books: MATEC Web of Conferences, Volume: 272, Volume: 01046. – 2019.
15. Fundamentals of building telecommunication systems and networks: Textbook for universities / Edited by V.N. Gordienko and V.V. Krukhmalev. – Moscow: Hotline – Telecom, 2004. – 510 p.
16. Kurilov I.A., Romashov V.V., Zhiganova E.A., Romanov D.N., Vasilyev G.S., Kharchuk S.M., Surzhik D.I. Methods of analysis of radio devices based on functional approximation // Radio engineering and telecommunication systems. 2014. No. 1 (13). pp. 35-49.
17. Garg, D. K. . (2022). Understanding the Purpose of Object Detection, Models to Detect Objects, Application Use and Benefits. International Journal on Future Revolution in Computer Science &Amp; Communication Engineering, 8(2), 01–04. https://doi.org/10.17762/ijfrcsce.v8i2.2066
18. Vasilyev G.S., Kurilov I.A., Kharchuk S.M., Surzhik D.I. Analysis of dynamic characteristics of the nonlinear amplitude-phase converter at complex input influence. //2013 International Siberian Conference on Control and Communications, SIBCON 2013 - Proceedings. 2013.
19. Surzhik D.I., Vasilyev G.S., Kuzichkin O.R. Modeling the dynamic properties of communication channels in UAV-based networks based on spectral piecewise linear approximation method / International Journal of Engineering Research and Technology. Volume 13, Issue 12. – 2021. – Pp. 4653-4657(Scopus).

20. Vasilyev G.S., Kurilov I.A., Kharchuk S.M., Surzhik D.I. Analysis of dynamic characteristics of the nonlinear amplitude-phase converter at complex input influence / 2013 International Siberian Conference on Control and Communications, SIBCON 2013 - Proceedings2013, №66936412013. - International Siberian Conference on Control and Communications, SIBCON 2013; Krasnoyarsk; Russian Federation; 12 September 2013 to 13 September 2013; CFP13794-CDR; Code 102462.
21. A. Chawla, "Phishing website analysis and detection using Machine Learning", Int J Intell Syst Appl Eng, vol. 10, no. 1, pp. 10–16, Mar. 2022.
22. Gonorovsky I.S. Radio engineering circuits and signals: Textbook for universities. – 4th ed. - Moscow: Radio and Communications, 1986. – 512 p.
23. M. . Parhi, A. . Roul, B. Ghosh, and A. Pati, "IOATS: an Intelligent Online Attendance Tracking System based on Facial Recognition and Edge Computing", Int J Intell Syst Appl Eng, vol. 10, no. 2, pp. 252–259, May 2022.
24. Bronstein I.N., Semendyaev K.A. Handbook of mathematics for engineers and students of higher education institutions – Ed. 9th stereotype - Moscow State Publishing House of Physical and Mathematical Literature. – 1962. – 608 p.